Journal of Applied Fluid Mechanics, Vol. 10, No. 1, pp. 41-53, 2017.
Available online at www.jafmonline.net, ISSN 1735-3572, EISSN 1735-3645.
DOI: 10.18869/acadpub.jafm.73.238.26331

Effect of Reverting Channels on Heat Transfer Performance of Microchannels with Different Geometries

M. Farzaneh, M. R. Tavakoli† and M. R. Salimpour

Department of Mechanical engineering, Isfahan University of Technology, Isfahan, 84156-83111, Iran.

†*Corresponding Author Email: mrtavak@cc.iut.ac.ir*

(Received March 24, 2016; accepted June 12, 2016)

ABSTRACT

This study investigated the effect of reverting microchannels inside a heat sink on increase of cooling rate as well as the effect of their different configurations on maximum temperature and pressure drop. Based on the convection heat transfer mechanism, selection of the embedded microchannels' configurations including circular, square and triangular ones, was studied for geometric optimization of the discussed heat sinks. The goal was to minimize the thermal resistance through optimizing the geometries. The volume ratio ϕ was defined as the ratio of the volume taken up by microchannels to the solid volume (portion of the heat sink not occupied by microchannels) and was considered as 0.05. According to the results, in addition to obtaining a more uniform temperature distribution, reverting channels remarkably reduced the maximum temperature. Moreover, the heat sink with square shape showed less thermal resistance as compared to the other two geometries.

Keywords: Geometrical optimization; Convective cooling; Constructal theory; CFD.

NOMENCLATURE

Be	dimensionless pressure drop
D_h	hydraulic diameter
k	thermal conductivity
$\dot{m}$	mass flow rate
P	pressure
R	$D_h/2$
ΔP	pressure drop
q''	heat flux
T	temperature
μ	dynamic viscosity
α	thermal diffusivity
ν	kinematic viscosity
ρ	density
ϕ	volume ratio
ave	average

Subscripts

f	fluid
in	inlet
out	outlet
s	solid

Superscripts

(~)	dimensionless

1. INTRODUCTION

Optimizing the fluid path line and the heat transfer has a remarkable effect on the conservation of energy resources. It improves total efficiency on the one hand and decreases costs on the other hand. In recent decades, many techniques have been developed to improve the thermal performance of different systems using heat transfer rate analysis such as Dewan *et al.* (2004), Laohalertdecha *et al.* (2007) and Murshed *et al.*(2011). The use of small channels and utilization of nanoscale sizes are approaches for improving heat transfer rate in channels that has been received great attentions in recent years. The use of forced flow inside microchannels is a method suggested for cooling electronic parts generating high temperatures. This idea was first put forward when Tuckerman *et al.* (1981) stated that the use of small-diameter channels is useful for cooling electronic circuits. They stated that as diameter decreases heat transfer coefficient increases. They showed that it is

possible to increase heat transfer coefficient of microchannels by 40 times compared the conventional heat exchangers. Wrisberg *et al.* (1992) carried out a 2D study on fluid flow and heat transfer rate assuming a hydrodynamically and thermally developed current inside the microchannels. Considering a thermal distribution, they numerically studied the heat transfer in liquid and surrounding solid and presented a design algorithm for the studied heat exchangers. Fedorv *et al.* (2000) applied the Navier-Stokes equations in the incompressible and laminar condition and presented a 3D model for heat absorbing microchannels.

Technological advances have introduced higher heat transfer capability as an important factor in designing micro-scaled systems. The configuration of microchannels has a tangible effect on the heat transfer rate. Constructal theory is an approach for optimizing the geometric features of microchannels. It concentrates on producing optimized constructs of currents. A system designer collects the components of a system and tries to optimize their configuration in order to achieve the maximum possible performance. This theory is based on the configuration of currents in nature. Concentrating on geometric optimization, it was introduced for the first time by Bejan *et al.* (1997) and has been widely studied in different fields till now. The outcome of this theory is that the shape of a system and its internal currents are not developed in random. Instead, optimization is used to achieve a better performance. Thus, it develops and evolves over time. The wide application of this theory has not been limited to heat transfer field, and it has been used in different fields such as fluid flow Wechsatol *et al.* (2001) and Gosselin *et al.*(2005), power distribution Arion *et al.* (2003), transportation Bejan *et al.* (2007) and biology Heitor *et al.* (2006) and Bejan *et al.* (2010), etc.

Pan *et al.* (2015) experimentally studied and optimized different structures of microchannels used in methanol steam reactor. They studied the effects of both cross-section and configuration and concluded that reactor efficiency depends on configuration more than cross-section.

Based on the constructal theory, wechsatel *et al. (*2003) developed convectional tree networks for cooling of heat generating disk-shaped parts. The aim of optimized designing of the structures was to achieve tree-like configuration with the minimum possible resistance against flow on the one hand and the minimum possible thermal resistance on the other hand. They showed, however, that the addition of bifurcations in several stages decreases the thermal resistance more than radial distribution.

Ramiar *et al.* (2012) numerically solved the conjugate heat transfer of a nanofluid in a 2D microchannel and investigated the effect of Reynolds number, nanoparticle conductivity. In another work, Kaya (2016) investigated the effects of ramification length and angle on pressure drop and heat transfer in a ramified microchannel. He showed that maximum temperature inside the ramified microchannel increases with increase of ramification length.

Bello-Ochende *et al.* (2007) studied the geometric optimization of a 3D heat sink numerically using the finite element method. In their study, microchannel had a variable cross-sectional area. The numerical results revealed that the degree of freedom has higher effect on the maximum temperature. In this way, optimum geometric properties were obtained.

Ghaedamini *et al.* (2011) used radial microchannels and studied the cooling of a circular disk using force convection approach. In their suggested microchannel network, fluid collecting network was used to increase heat transfer rate. The effect of the number of bifurcations on pressure drop and heat transfer was studied in that study. It was shown that as the number of bifurcations increases, temperature is distributed more uniformly while temperature gradient decreases. This suggests that the highest complexity does not necessarily mean the best performance. Silva *et al.* (2004) studied the cooling of disk-shaped parts with internal heat generation. They studied the configuration of blades embedded inside the disk and attached to its side. In optimal condition, geometric parameters and thermal resistance were shown as a function of the ratio of thermal conductivity coefficient of the two materials, the ratio of the weight of two materials, and the number of circular sectors in related graphs.

Wang *et al*. (2015) studied the electroosmotic flow of Newtonian fluids through a semicircular microchannel and found an analytical solutions. They found that the electroosmosis flow driven by an alternating electric field is quasi-periodic in time. Niazmand *et al*. (2010) studied the rarefaction effects in fully developed flow in rectangular microchannels with a prescribed uniform wall heat flux in the slip-flow regime and observed reductions in the friction coefficient are in the entrance region due to rarefaction effects. In addition, similar works in which usage of microchannels played important roles were published in Qazi Zade *et al.* (2015) and Hamedi *et al.* (2016). Farzaneh *et al.* (2016) investigated convective cooling of a square shape piece using dendritic microchannels with/without loops within the platform of constructal theory. Their computed results showed that the number of branches significantly affects the maximum dimensionless temperature and its uniformity and use of dendritic network and T-shaped branches, are preferred. In another work, Shadlaghani *et al.* (2016) numerically investigated an appropriate pattern to allow for a better design of the extended surfaces used in triangular heat sinks. Their goal was to achieve the best architecture of perforated fins with considering maximum heat dissipation rate and minimum pressure drop.

In this study the effect of reverting channels inside a heat sink on increasing the cooling rate and the effect of different configurations of microchannels on maximum temperature and pressure drop was investigated.

For geometric optimization of the studied heat sink,

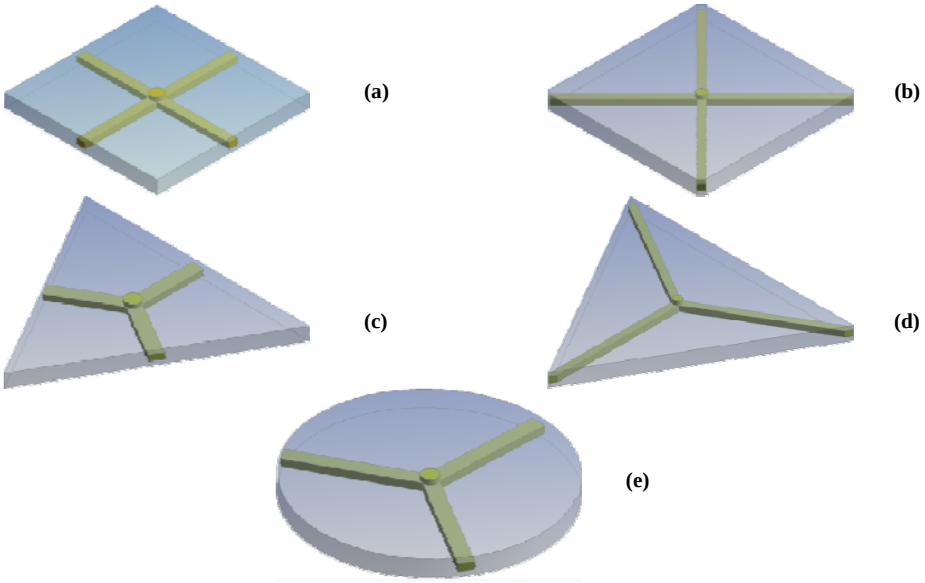

Fig. 1. Distribution of fluid inside the heat sink without collection.

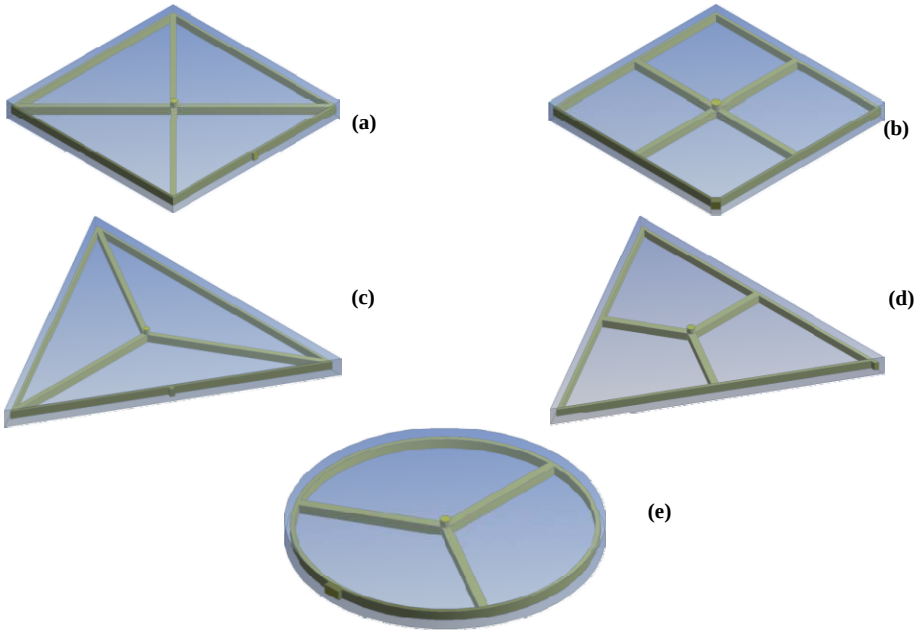

Fig. 2. Fluid collection by the collecting ring located in heat sink periphery.

three circular, square and triangular cross-sections with the constraint of constant volume ratio were studied. (The volume ratios φ was defined as the ratio of the volume taken up by microchannels to the portion of the heat sink which not occupied by the microchannels)

2. MODEL AND NUMERICAL ANALYSIS

Figure. 1 shows a 3D heat sink with fluid distribution channels. This study assesses the configuration of microchannels and their optimization as well as the geometric optimization of the studied heat sink under heat flux in order to achieve the maximum heat transfer rate. Three cross sections of heat sink (i.e. circular, triangular and square) were studied for the geometric optimization purposes. The constant volume of the heat sink and the ducts embedded inside were considered as the constraints of the studied geometries. Heat is transferred to the bottom heat absorbing surface through the heat generating surfaces and is then directed through silicon-made solid surfaces with a high coefficient of conductivity. Then, it is dissipated by coolant fluid flowing through microchannels. According to Fig. 1, microchannels can be distributed along the diameters or along the mid-side of triangular and square heat sinks. The

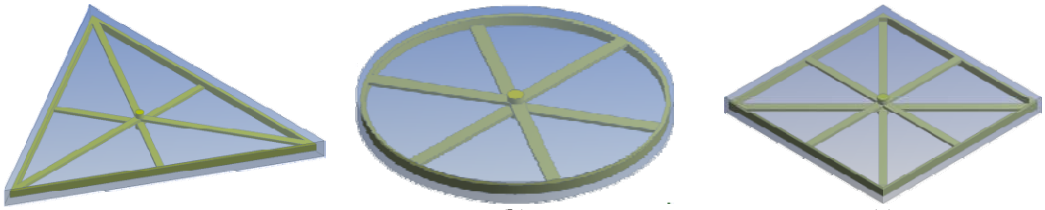

(a) **(b)** **(c)**

Fig. 3. Microchannels configurations with reverting paths.

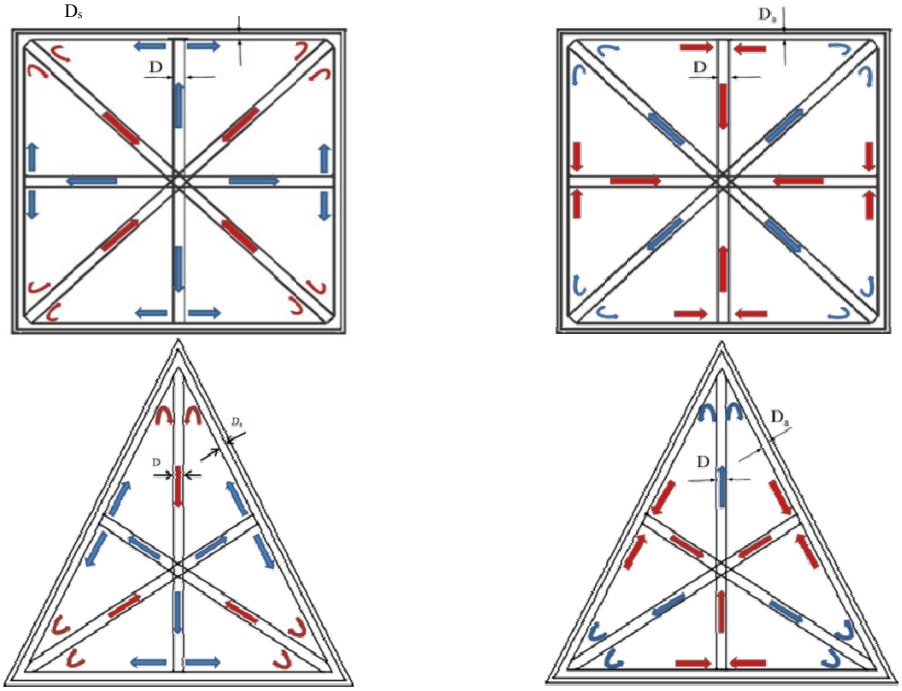

Fig. 4. Distribution/collection of fluid along diameter/center and vice versa.

coolant fluid enters from the center of heat sinks and flows inside the part through the embedded microchannels and exit from the mid-side (Fig. 1(a) and 1(c)) or corners (Fig. 1(b) and 1(d)) of the heat sinks.

The distributed fluid can be collected and reused to increase the heat transfer rate. Two configurations can be adopted for this purpose. In the first configuration, fluid enters from the center of heat sink and is collected from periphery (Fig. 2). In the second configuration, it enters from the center, cools it down through reverting channels and then leaves the heat sink from its center (Fig. 3). According to Fig. 2, to collect fluid from periphery, the distributed coolant fluid enters from the heat sink center and is directed towards outside through a ring located at the end of the distribution path.

In triangular and square shape heat sinks, there are two possible locations for the ring. In the first location, the leaving channel is located at one of the corners of the collecting ring (Fig.2(b) and 2(d)) while in the second location, it is located at the mid-side of the collecting ring (Fig.2(a) and 2(c)).

In the second configuration, reverting channels located beneath the inlet channel can be used for this purpose (Fig.3). In this case, fluid enters from the center of top surface, flows through microchannels and leaves the heat sink from the bottom surface through reverting channels.

Similar to previous case, there are again two possible scenarios for distributing fluid inside triangular and square heat sinks equipped with reverting microchannels. In the first case, fluid enters along the channel diameter and is collected in the mid-side of the bottom surface through reverting channel network and finally leaves the heat sink from its center (Fig. 4(b) and 4(d)). In the second case, fluid enters from the center of the channels and enters to the heat sink through the channels embedded in mid-sides and then is collected along diameter through reverting microchannel network embedded beneath the heat sink and finally leaves that from its center (Fig. 4(a) and 4(c)).

In the second configuration, reverting channels located beneath the inlet channel can be used for

Table 1 Brief classification of different discussed geometries

Channel Distribution	Case number	figure number
Distribution alongside center without collection, square heat sink	Case1	Fig. 1(a)
Distribution alongside diameter without collection, square heat sink	Case2	Fig. 1(b)
Distribution alongside center without collection, triangular heat sink	Case3	Fig. 1(c)
Distribution alongside diameter without collection, triangular heat sink	Case4	Fig. 1(d)
Distribution alongside radius without collection, circular heat sink	Case5	Fig. 1(e)
Distribution alongside center with collecting ring, square heat sink	Case6	Fig. 2(a)
Distribution alongside diameter with collecting ring, square heat sink	Case7	Fig. 2(b)
Distribution alongside center with collecting ring, triangular heat sink	Case8	Fig. 2(c)
Distribution alongside diameter with collecting ring, triangular heat sink	Case9	Fig. 2(d)
Distribution alongside radius with collecting ring, circular heat sink	Case10	Fig. 2(e)
Distribution alongside center with reverting channel, square heat sink	Case11	Fig. 4(a)
Distribution alongside diameter with reverting channel, square heat sink	Case12	Fig. 4(b)
Distribution alongside center with reverting channel, triangular heat sink	Case13	Fig. 4(c)
Distribution alongside diameter with reverting channel, triangular heat sink	Case14	Fig. 4(d)
Distribution alongside radius with reverting channel, circular heat sink	Case15	Fig. 3(b)

this purpose (Fig.3). In this case, fluid enters from the center of top surface, flows through microchannels and leaves the heat sink from the bottom surface through reverting channels. Table 1 briefly summarizes all the mentioned cases in this paper.

In order to compare the effect of different configurations on the dimensionless maximum temperature, the same boundary conditions were applied in all cases. The ratio of volume taken up by the microchannels to the remaining volume of disk was introduced as the volume ratio shown by ϕ. As a constraining condition, ϕ has the same value in all cases and equals to 0.05.

$$\phi = \frac{volume\ taken\ up\ by\ the\ microchannels}{remain\ volume\ of\ disk} \qquad (1)$$

Now, the effect of reverting channels on the cooling performance of microchannels is studied. All aforementioned cases were studied in the following. D_a / D (channel diameter outside ring to channel diameter inside the heat sink) was a given value in this study and equals to 0.5. It does not necessarily mean an optimized value.

The hydraulic diameter of the studied microchannels was greater than 10 μm. According to the studies by Obot (2004), the condition of continuum environment is satisfied for water with the mentioned hydraulic diameter. The Navier-Stokes and energy equations were coupled with solid heat transfer equation (that controls transfer processes very well), and the developed system was studied to analyze flow and heat transfer in a steady, laminar and incompressible condition with constant fluid and solid properties. Table 2 shows the properties of water and silicone. Moreover, the volume ratio ϕ and the total volume of network is kept constant in every stage of analysis. A numerical analysis approach was used to examine pressure drop, temperature distribution, and heat transfer rate in every case. Results are shown as dimensionless values. According to typical assumptions, conservation of mass and conservation of momentum equations are stated as follows:

$$\nabla.\bar{U} = \frac{\partial u}{\partial x} + \frac{\partial v}{\partial y} + \frac{\partial w}{\partial z} = 0 \qquad (2)$$

$$(\bar{U}.\nabla\bar{U}) = -\nabla P + \mu\nabla^2\bar{U} \qquad (3)$$

Laplace operator is defined as $\nabla^2 = \partial^2/\partial x^2 + \partial^2/\partial y^2 + \partial^2/\partial z^2$ .Conservation of energy equation for the fluid phase is defined as:

$$\rho_f C_{p,f}(\vec{U}.\nabla T) = k_f \nabla^2 T \qquad (4)$$

While the equation of heat transfer for solid phase is defined as:

$$k_s \nabla^2 T = 0 \Rightarrow \nabla^2 T = 0 \qquad (5)$$

Standard no-slip condition is applied on channel walls. Constant mass flow rate boundary condition is applied in the inlet of the channel. Outlet pressure and inlet temperature were considered as $P_{out} = 1atm$ and $T_{in} = 300K$ for simplification purposes. Thermal flux imposed from the bottom side is derived from the following equation:

$$k_s \frac{\partial T}{\partial y} = -q'' \qquad (6)$$

and other surfaces are non-conductor. Regarding the continuum of temperature and heat flux in fluid and

solid interface, we have:

$$-k_s \left.\frac{\partial T_s}{\partial n}\right|_{\Omega} = -k_f \left.\frac{\partial T_f}{\partial n}\right|_{\Omega} \quad (7a)$$

$$T_s = T_f \quad (7b)$$

Where k_f and k_s are fluid and solid thermal conductivity coefficients, respectively. Ω is the normal vector of fluid and solid interface.

Table 2 Properties of silicone and water

Property	silicone	water
Density, ρ , (kg/m3)	2330	998
Thermal conductivity, k, (W/mK)	125	0.6069
Specific heat capacity, Cp, $(kJ / kg\ K)$	700	4.18
Dynamic viscosity, μ , (Pa s)	-	8.899

Dimensionless variables are defined as follows:

$$\tilde{x},\tilde{y},\tilde{z} = \frac{x,y,z}{R} \quad (8)$$

$$\tilde{T} = \frac{(T - T_{in})}{q'' R / k_f} \quad (9)$$

$$Be = \frac{(P_{in} - P_{out})R^2}{\alpha_f \mu} \quad (10)$$

$$\tilde{m} = \frac{\dot{m}}{\alpha_f \rho_f R\ Pr} \quad (11)$$

Where, Be is dimensionless pressure drop based on Petrescu (1994) and Bhattacharjee *et al.*(1988) definitions.

2.1 Validation

This study was validated by comparing its results on a circular heat sink with the results published by Ghaedamini in Fig. 5. Both studies applied the same boundary conditions and assumptions, including the geometric constraints implying that radial configuration have been studied for two geometric properties: total number of bifurcations and cross-section area of the geometry. Radial configurations with 3, 4, 6 and 8 bifurcations were used for this purpose. The comparisons revealed that for the same number of bifurcations, there is a good agreement between two studies in terms of dimensionless maximum temperature and pressure drop. Note that the results reported by Ghaedamini *et al.* were verified by those obtained by Wang *et al.* (2006).

2.2 Grid Independency Analysis

This numerical analysis predicts the convection heat transfer and pressure drop in a reverting microchannel network with different geometries through solving 3D Navier-Stokes and energy equations for an incompressible fluid with constant properties. Irregular meshing method was used to mesh the studied geometries. This method can be easily applied in complex geometries. Due to a high temperature gradient, a fine grid was applied on microchannel sides compared with other zones. Four grid were studied to investigate the grid independency of numerical solutions,. In each grif, the number of elements was incrementally raised until the variatons in T_{max} becomes less than 1%. Table 3 shows a sample of grid independency analysis when bifurcation-free micro channle is used.

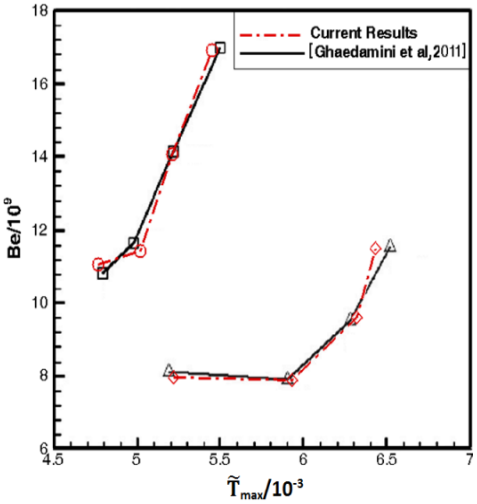

Fig. 5 Comparison of dimensionless temperature contours in a circular heat sink with those obtained by Ghaedamini *et al.*

Table 3 Grid independency

Number of elements	412907	672357	953896	1480969
T_{max}	365.4	360.7	357.5	356.8

3. Results And Discussion

3.1 Fluid Distribution without Collection

In this case, fluid enters from the center of the heat sink into the microchannel and leaves it along the same direction after distribution throughout the heat sink. In square and triangular heat sinks, distribution channels can be designed at mid-sides or along the diameter. According to the temperature distribution contours, the maximum temperature happens at the farthest zone from fluid distribution channels. Temperature distribution contour (Fig. 6) shows that in the case of radial configuration for the same channel volume, maximum dimensionless temperature has a lower value, and temperature is distributed more uniformly. The reason is that in the case of radial distribution, surface to volume ratio

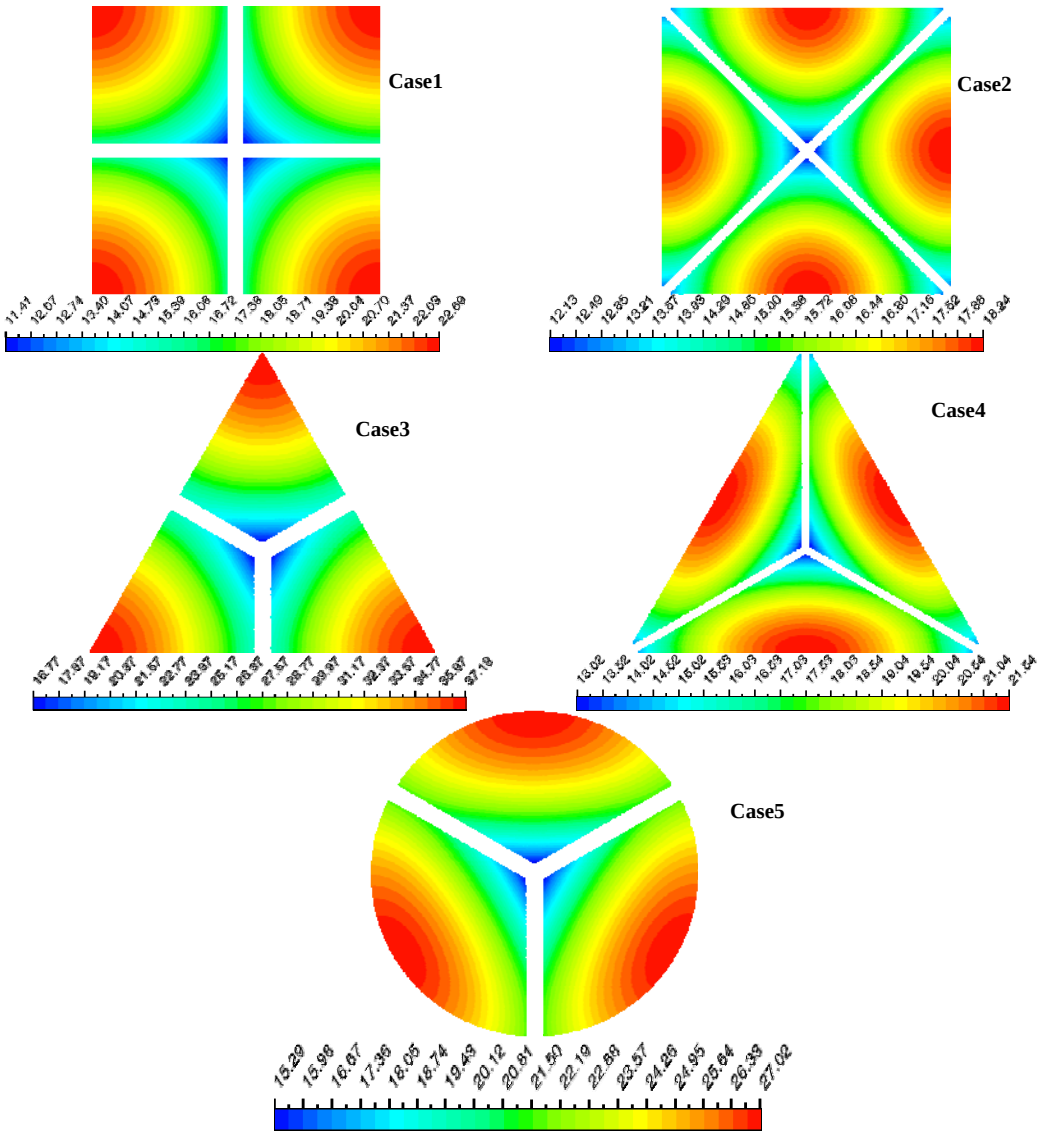

Fig. 6. Contour of dimensionless temperature distribution for case 1 to case 6.

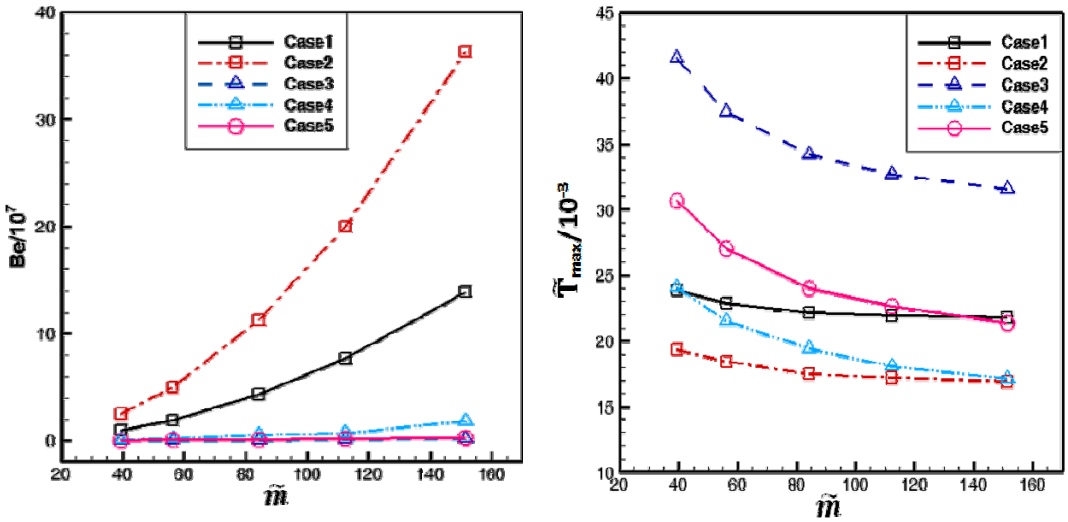

Fig. 7. Dimensionless temperature and pressure drop for case 1 to case 5 for different flow rates.

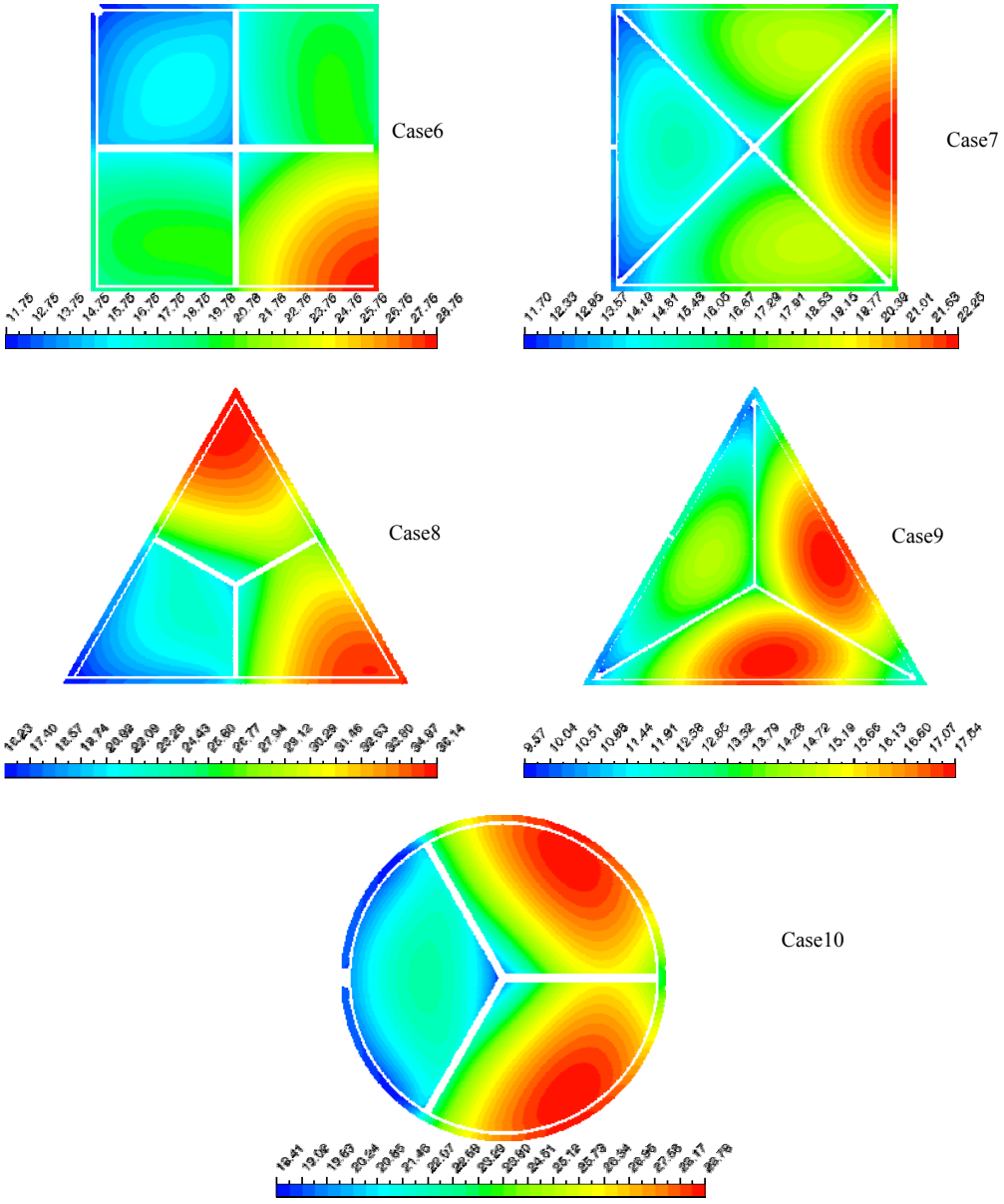

Fig. 8. Dimensionless temperature distribution contour for case6 to case10.

of microchannel (S/V) is higher than that of the case where the distribution occurs along sides. Table 4 shows S/V ratio in the above samples:

Table 4 S/V ratios of microchannels for case1 to case5

Case number	Case1	Case2	Case3	Case4	Case5
s/v	0.1116	0.1288	0.0968	0.1258	0.1055

In the triangular geometry, the S/V ratio had a lower value in both fluid distribution cases compared with the same geometry in square heat sink while microchannels and heat sinks have the same volume in all cases. This can justify the increased temperature in triangular geometry of microchannel.

Figure. 7 shows the average dimensionless maximum temperature and average pressure drop for different flow rates. According to expectations, the average maximum temperature decreased as flow rate increases while pressure drop increased by 10 times as much as before. Since increase in temperature was slightly decreased with increase in flow rate, and in contrast, it significantly increased by pressure drop, increased flow rate is not always justifiable. In these configurations, pressure drop was caused by the pressure drop in the pipes. According to the Poiseuille flow, the relationship between pressure drop, mass flow rate and geometric properties of a smooth channel is defined by the following equation:

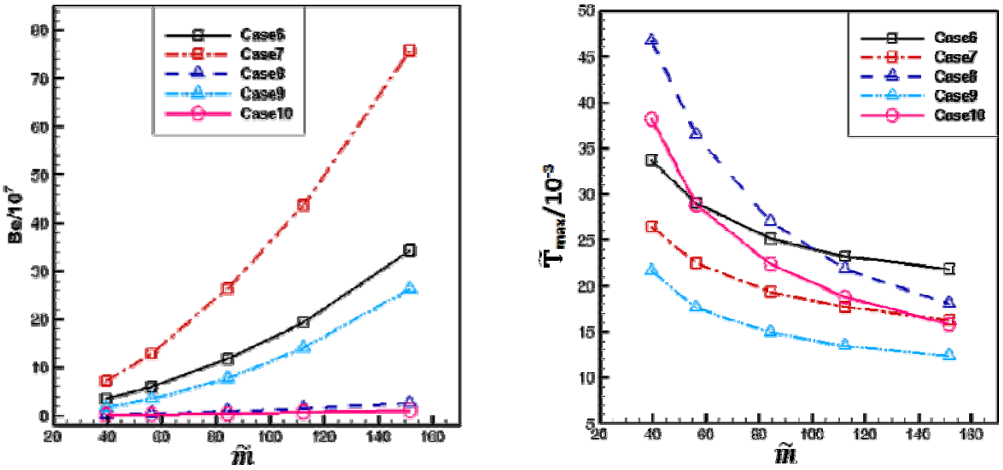

Fig. 9. Dimensionless temperature and pressure drop in case 6 to case 10 at different flow rates.

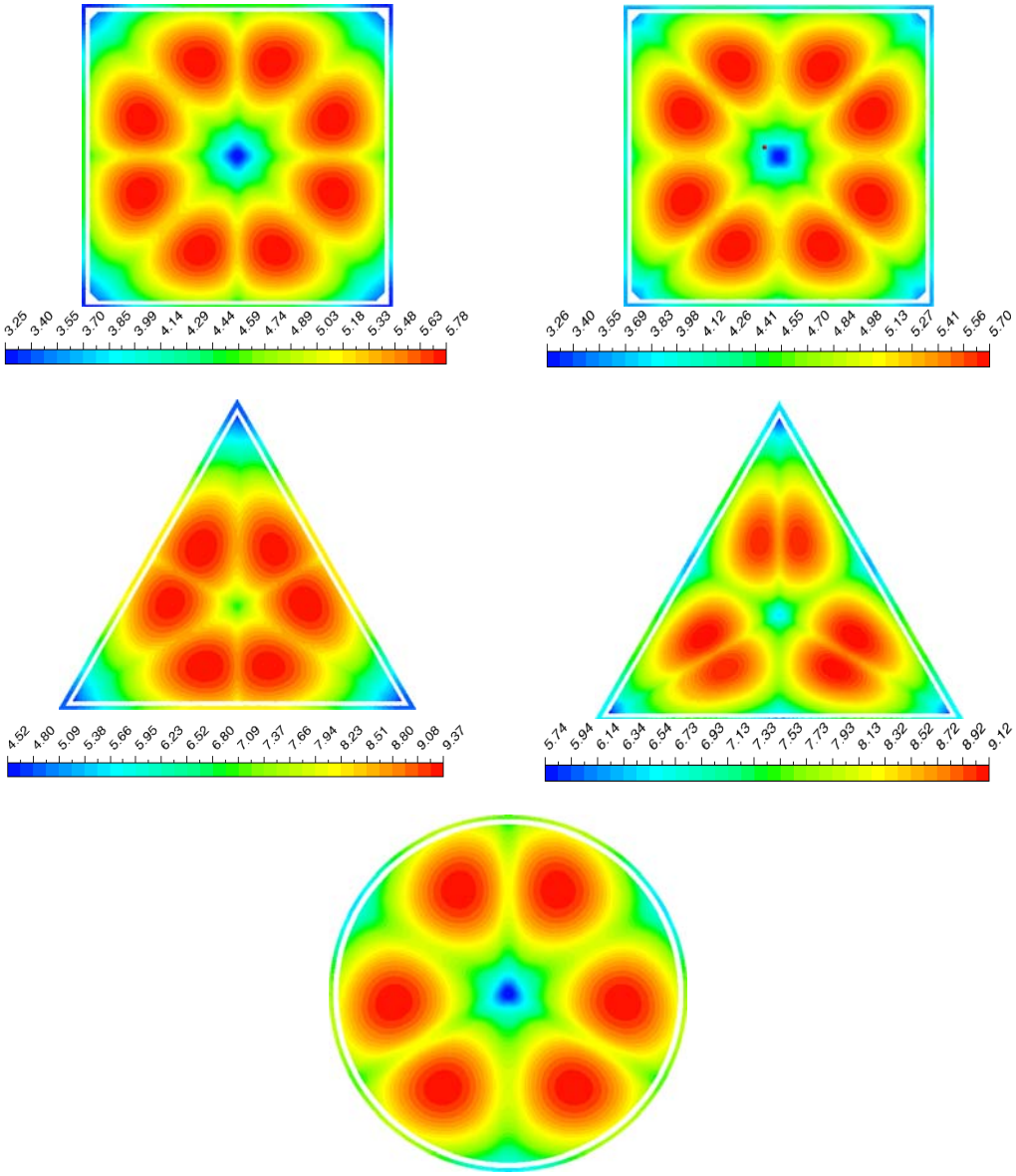

Fig. 10. Temperature distribution contour for case 11 to case 15.

$$\Delta P_{distributed} = 2\nu P_0 \frac{\dot{m}L}{d_h^2 A} \quad (12)$$

Since in mid-side configuration, the length is shorter, this design has lower pressure drop as compared to radial configuration.

3.2 Fluid Collection using Collection Ring

When a collecting ring is used, fluid tends to flow through a path with the minimum pressure drop. Therefore, less fluid flows through the path with the maximum length and there will be a higher mass flow rate in the paths closer to the outlet. In addition to the distributed pressure drop, there is a local pressure drop due to the elbows in fluid path line. In general, pressure drop inside a microchannel, which includes both local and distributed pressure drops, is derived from relationship (13) as follows:

$$\Delta P = \Delta P_{distributed} + \Delta P_{local} \quad (13)$$

According to Fig. 8, despite expectations, the use of collecting ring in the square heat sink not only did not decrease dimensionless maximum temperature but also increased it. The reason is that between two known points (inlet and outlet points) fluid tends to flow through a route with a minimum pressure drop. Therefore, in a route with a higher pressure drop, the fluid velocity decreases and it flows in a very small amount. This increases temperature in regions that are closer to the microchannels. Therefore, when a collecting ring is used, the maximum temperature is higher than that of previous cases.

Fig. 9 shows pressure drop and average dimensionless maximum temperature curves for case 6 to case 10. According to this figure, as flow rate increases average maximum temperature decreases while pressure drop increases significantly. In the case of triangular heat sink and a collecting ring, when fluid flows through the ring it experiences lower pressure drop as compared to the square heat sink. The reason is shorter length of flow path. Thus, temperature is improved compared with previous cases while no difference is seen in circular heat sink. Table 5 shows S/V ratio of microchannels in case6 to case10.

Table 5 S/V ratios of microchannels for case6 to case10

Case No.	*Case6*	*Case7*	*Case8*	*Case9*	*Case10*
s/v	0.1936	0.2108	0.1892	0.2158	0.1775

According to this table, the higher S/V ratio, the higher the rate of heat transferred to coolant fluid and the lower the maximum temperature inside the heat sink. S/V ratio was 0.2532, 0.2256 and 0.2358 for square, circular and triangular heat sinks respectively. According to the temperature contours (Fig. 10), in case of using microchannel for cooling purposes, a more uniform temperature distribution is obtained compared with previous cases. This figure indicates the superiority of center collection approach because in this case, the maximum dimensionless temperature of the heat sink decreases significantly as compared to side collection approach. The difference between average temperature of heat sink and the maximum temperature can be considered a proper measure for uniform temperature distribution. The best design for fluid distribution is the case in which the average temperature in the heat sink approaches the maximum temperature. According to Fig. 11, the use of collecting ring results in a more uniform temperature distribution across the heat sink.

However, an increased flow rate significantly increases the pressure drop while temperature gradient decreases with a low speed. This means that any increase in flow rate does not necessarily an economical**.**

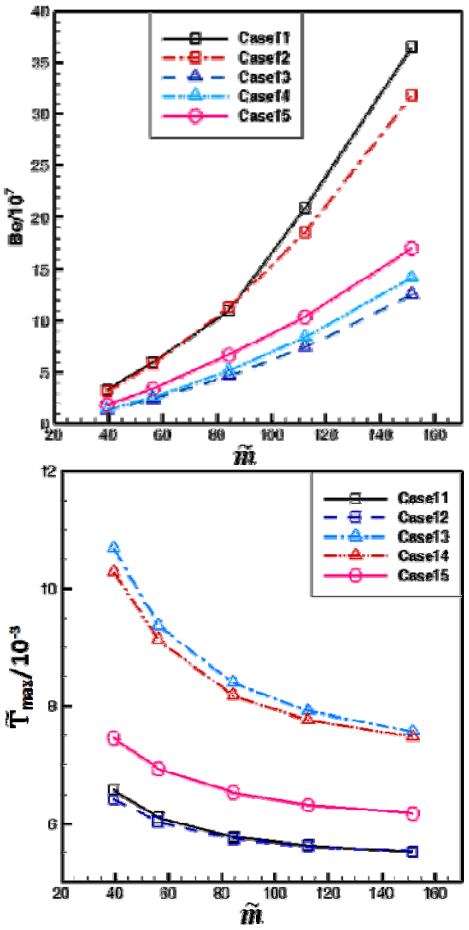

Fig. 11. Average maximum temperature and dimensionless pressure drop in case11 to case15 at different flow rates.

When we speak about the best thermal model, both maximum temperature and uniform temperature distribution factors should be studied at the same time. Figure. 12 shows the ratio of average temperature to the maximum temperature inside the heat sink for different flow rates in all the studied cases. As mentioned before, when the maximum

temperature is T_{max}, the optimal case is the case in where the whole heat sink is at temperature T_{max}. According to the diagrams in Fig. 12, when microchannels are added to square geometry design, average to maximum temperature ratio approaches 1 at different flow rates leading to a more optimal condition.

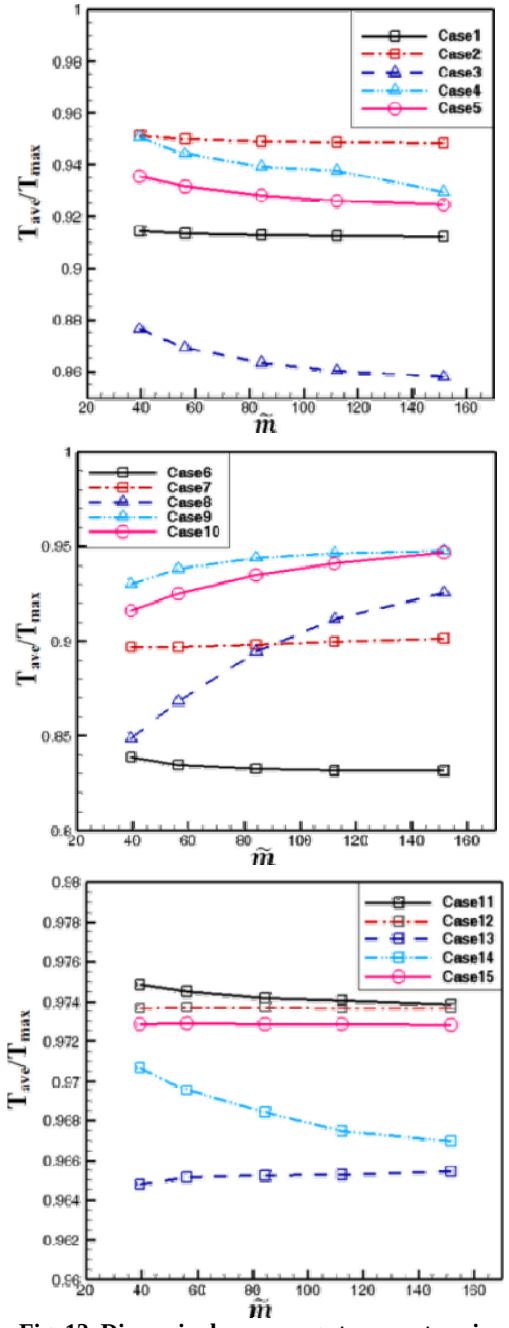

Fig. 12. Dimensionless average temperature in case1 to case15 at different flow rates.

3.3 Use of Reverting Microchannel Network

A notable conclusion that can be derived from the obtained results is that temperature has an asymmetric distribution in the mentioned configurations. When we speak about the best thermal design, both maximum temperature and uniform temperature distribution factors should be studied at the same time. In fact, when the maximum temperature of a heat sink is T_{max} the optimal case is the case in which whole the heat sink works at temperature T_{max} or, in other words, there is a uniform temperature distribution. To achieve a more uniform temperature distribution, the distributed fluid can be reused for cooling purposes. Reverting channels embedded beneath the inlet channel can be used for this purpose. In the studied cases, the S/V ratio was 0.2532, 0.2256 and 0.2358 for square, circular and triangular heat sinks respectively. According to the temperature contours (Fig. 10), in case of using microchannel for cooling purposes, a more uniform temperature distribution is obtained compared with previous cases. This figure indicates the superiority of center collection approach because in this case, the maximum dimensionless temperature of the heat sink decreases significantly as compared to side collection approach.

The difference between average temperature of heat sink and the maximum temperature can be considered a proper measure for uniform temperature distribution. The best design for fluid distribution is the case in which the average temperature in the heat sink approaches the maximum temperature. According to Fig. 11, the use of collecting ring results in a more uniform temperature distribution across the heat sink. However, an increased flow rate significantly increases the pressure drop while temperature gradient decreases with a low speed. This means that any increase in flow rate does not necessarily an economical.

When we speak about the best thermal model, both maximum temperature and uniform temperature distribution factors should be studied at the same time. Figure. 12 shows the ratio of average temperature to the maximum temperature inside the heat sink for different flow rates in all the studied cases. As mentioned before, when the maximum temperature is T_{max}, the optimal case is the case in where the whole heat sink is at temperature T_{max}. According to the diagrams in Fig. 12, when microchannels are added to square geometry design, average to maximum temperature ratio approaches 1 at different flow rates leading to a more optimal condition.

4. CONCLUSION

To improve the thermal performance of a silicone made piece, different configurations of microchannels with different geometries were studied. Hereby, three geometries were numerically studied at a constant volume of microchannels. According to the results, in different configurations the use of reverting channel network as well as distributing fluid along diameter has a considerable effect on the dimensionless maximum temperature and uniform temperature distribution due to higher

S/V ratio. However, numerical results suggested that square geometry shows the least thermal resistance. Another conclusion was that the use of reverting microchannels reduced the maximum temperature and increased the pressure drop. Reverting channels shifted the maximum temperature zone from sides to the surface center. In addition to a remarkable decrease in the dimensionless maximum temperature, the addition of reverting microchannels resulted in more uniform temperature distribution.

REFERENCE

Arion, A., A. Cojocari and A. Bejan (2003). Constructal tree shaped networks for the distribution of electrical power. *Energy Conversion and Management* 44(6), 867-891.

Bejan, A. (2000). Shape *and structure from engineering to nature,* Cambridge University Press, Cambridge, UK.

Bejan, A. and G. Merkx (2007). *Constructal Theory of Social Dynamics,* Springer Verlag, New York.

Bejan, A. and S. Lorente (2006). Constructal theory of generation and configuration in natureand engineering. *Journal of Applied Physics* 100.

Bejan, A. and S. Lorente (2010). The constructal law of design and evolution in nature. *Phil. Trans. R. Soc. B* 365(1545), 1335–1347.

Bello-Ochende, T., L. Liebenberg and J. P. Meyer (2007). Constructal cooling channels for micro-channel heat sinks. *International Journal of Heatand Mass Transfer* 50, 4141-4150.

Bhattacharjee, S. and W. L. Grosshandler (1988). The formation of wall jet near a high temperature wall under microgravity environment. *ASME National Heat Transfer Conference* 96, 711-716.

Dewan, A., P. Mahanta, K. S. Raju and P. S. Kumar (2004). Review of passive heat transfer augmentation techniques. *Journal of Power Energy* 218(A7), 509-527.

Farzaneh, M., M. R. Salimpour and M. R. Tavakoli (2016). Designof bifurcating microchannels with/without loops for cooling of square-shapedelectronic components. *Applied Thermal Engineering* 108, 581-595.

Fedorov, A. G. and R. Viskanta (2000). Three-dimensional conjugate heat transfer in the microchannel heat sink for lectronic packaging. *International Journal of Heat and Mass Transfer* 43, 399-415.

Ghaedamini, H., M. R. Salimpour and A.Campo, A. (2011). Constructal design of reverting microchannels for convective cooling of a circular disc. *International Journal of Thermal Science* 50, 1051-1061.

Gosselin, L. and A. Bejan (2005). Emergence of asymmetry in constructal tree flow networks. *Journal of Applied Physics* 98(10).

Hamedi, A., M. Shamshiri, M. Charmiyan and E. Shirani (2016). Investigation of nonlinear electrokinetic and rheological behaviors of typical non-newtonian iofluids through annular microchannels. *Journal of Applied Fluid Mechanics* 9, 367-378.

Heitor, A. and A. Bejan (2006) Constructal theory of global circulation and climate. *International Journal of Heat and Mass Transfer* 49, 1857-1875.

Kaya, F. (2016). Numerical investigation of effects of ramification length and angle on pressure drop and heat transfer in a ramified microchannel. *Journal of Applied Fluid Mechanics* 9, 767-772.

Laohalertdecha, S., P. Naphon and S. Wongwises (2007). A review of electrohydrodynamic enhancement of heat transfer. *Renew. Sust. Energy. Rev.* 11(5), 858-876.

Niazmand, H., A. M Jaghargh and M. Renksizbulut (2010). Slip-flow and heat transfer in isoflux rectangular microchannels with thermal creep effects. *Journal of Applied Fluid Mechanics* 3, 33-41.

Obot, N. T. (2004). Toward a better understanding of friction and heat/mass transfer in microchannels a literature review. *Microscale Thermophysical Engineering* 6, 155-173.

Pan, M, Q. Wu, L. Jiang and D. Zeng (2015). Effect of microchannel structure on the reaction performance of methanol steam reforming. *Applied Energy* 154, 416-427.

Petrescu, S. (1994). Comments on the optimal spacing of parallel plates cooled by forced convection. *International Journal of Heat and Mass Transfer* 37, 1283.

Qazi Zade, A., M. Renksizbulut and J. Friedman (2015). Ammonia decomposition for hydrogen production in catalytic microchannels with slip/jump effects. *Journal of Applied Fluid Mechanics* 8, 703-712.

Ramiar, A., A. A. Ranjbar and S. F. Hosseinizadeh (2012). Effect of axial conduction and variable properties on two-dimensional conjugate heat transfer of Al2O3-EG/water mixture nanofluid in microchannel. *Journal of Applied Fluid Mechanics* 5, 79-87.

Shadlaghani, A., M. R. Tavakoli, M. Farzaneh and M. R. Salimpour (2016). Optimization of triangularfins with/without longitudinal perforate for thermal performance enhancement. *Journal of Mechanical Science and Technology*, 30 (4), 1903-1910.

Silva, A., C. Vasile and A. Bejan (2004). Disc cooled with high conductivity inserts that extend inward from the perimeter.

International Journal of Heat and Mass Transfer 47, 4257-4263.

Sohel Murshed, S. M., C. A. Nieto de Castro, M. J. V. Lourenco, M.L.M. Lopes, F. J. V. Santos (2011). Review of boiling and convective heat transfer with nanofluids. *Renew. Sust. Energy Rev.* 15(5), 2342–2354.

Tuckerman, D. B. and R. F. Pease (1981). High-performance heat sinking for VLSI. *IEEE* 2, 126-129.

Wang, S., M. Zhao, X. Li and S. Wei (2015). Analytical solutions of time periodic electroosmotic flow in a semicircular microchannel. *Journal of Applied Fluid Mechanics* 8, 323-327.

Wang, X. Q., C. Yap and A. S. Mujumdar (2006). Laminar heat transfer in constructal microchannel networks with loops. *Journal of Electron Packaging* 128(3), 273-280.

Wechsatol, W., S. Lorente and A. Bejan (2001). Tree-shaped insulated designs for the uniform distribution of hot water over an area. *International Journal of Heat and Mass Transfer* 44, 3111-3123.

Wechsatol, W., S. Lorente and A. Bejan (2003). Dendritic convection on a disc. *International Journal of Heat and Mass Transfer* 46, 4381-4391.

Weisberg, A., H. Bau and J. Zemel (1992). Analysis of microchannels for integrated cooling. *International Journal of Heat and Mass Transfer* 35, 2465–2474.